# Enhanced surface transfer doping of diamond by $V_2O_5$ with improved thermal stability

Kevin G. Crawford' , Liang Cao, Dongchen Qi' , Alexandre Tallaire, E. Limiti, C. Verona, Andrew T. S. Wee, and David A. J. Moran

Citation: Appl. Phys. Lett. **108**, 042103 (2016); doi: 10.1063/1.4940749
View online: http://dx.doi.org/10.1063/1.4940749
View Table of Contents: http://aip.scitation.org/toc/apl/108/4
Published by the American Institute of Physics



# Enhanced surface transfer doping of diamond by $V_2O_5$ with improved thermal stability

Kevin G. Crawford,[1,a)] Liang Cao,[2,3] Dongchen Qi,[4,b)] Alexandre Tallaire,[5] E. Limiti,[6] C. Verona,[6] Andrew T. S. Wee,[3] and David A. J. Moran[1]
[1]*School of Engineering, University of Glasgow, Glasgow G12 8LT, United Kingdom*
[2]*High Magnetic Field Laboratory, Chinese Academy of Sciences, 350 Shushanhu Road, Hefei 230031, Anhui, People's Republic of China*
[3]*Department of Physics, National University of Singapore, 2 Science Drive 3, Singapore, Singapore 117542*
[4]*Department of Chemistry and Physics, La Trobe Institute for Molecular Science, La Trobe University, Melbourne, Victoria 3086, Australia*
[5]*LSPM-CNRS, Université Paris 13, Villetaneuse 93430, France*
[6]*Department of Industrial Engineering, "Tor Vergata" University, Rome 00173, Italy*

(Received 2 November 2015; accepted 14 January 2016; published online 27 January 2016)

Surface transfer doping of hydrogen-terminated diamond has been achieved utilising $V_2O_5$ as a surface electron accepting material. Contact between the oxide and diamond surface promotes the transfer of electrons from the diamond into the $V_2O_5$ as revealed by the synchrotron-based high resolution photoemission spectroscopy. Electrical characterization by Hall measurement performed before and after $V_2O_5$ deposition shows an increase in hole carrier concentration in the diamond from $3.0 \times 10^{12}$ to $1.8 \times 10^{13}\,cm^{-2}$ at room temperature. High temperature Hall measurements performed up to 300 °C in atmosphere reveal greatly enhanced thermal stability of the hole channel produced using $V_2O_5$ in comparison with an air-induced surface conduction channel. Transfer doping of hydrogen-terminated diamond using high electron affinity oxides such as $V_2O_5$ is a promising approach for achieving thermally stable, high performance diamond based devices in comparison with air-induced surface transfer doping. © *2016 AIP Publishing LLC*.
[http://dx.doi.org/10.1063/1.4940749]

Diamond has a wide electronic band-gap of 5.47 eV, combined with an intrinsically high breakdown field of 10 MV/cm, an exceptional thermal conductivity of >20 W/cm K, and a hole saturation velocity of $0.85–1.2 \times 10^7\,cm\ s^{-1}$, which makes it very attractive for high frequency, high power applications based on devices such as field effect transistors (FETs).[1] The robust nature of diamond may enable devices which operate beyond the capabilities of conventional solid-state devices in terms of power handling capacity and operating environment. However, conventional substitutional doping in diamond remains challenging which has limited its potential exploitation for electronic applications.[2] Alternatively, surface transfer doping of hydrogen-terminated diamond (H-diamond) shows great promise. This doping process traditionally relies upon interfacial electron transfer between the diamond valence band and favourable energy states provided by atmospheric molecules dissolved in a water layer naturally adsorbed on the diamond surface.[3] High frequency devices based on H-diamond exposed to air have already been demonstrated with the fabrication of FETs[4,5] showing a cut-off frequency ($f_T$) of up to 53 GHz[6] and a maximum frequency ($f_{max}$) of 120 GHz.[7] However, the stability of this atmospheric layer upon which the transfer doping process relies has been a significant limiting factor in the production of high-power handling and robust operation devices, with a maximum high power operation of 2 W/mm at 1 GHz reported thus far.[8]

In recent studies, substitution of the surface atmospheric layer with solid-state surface acceptors for efficient surface transfer doping of H-diamond has been actively pursued.[2] The fullerene molecule $C_{60}$[9] and its fluorinated variants $C_{60}F_{48}$[10] and $F_4$-TCNQ[11] are well known to have a high electron affinity (EA) and have been demonstrated to induce surface transfer doping on H-diamond. These organic materials, however, still demonstrate limited stability in air, despite attempts to encapsulate them.[12] A more recent approach has demonstrated improved stability up to 550 °C in air[13] through atomic layer deposition (ALD) of $Al_2O_3$ on H-diamond, resulting in carrier concentrations between $8.0 \times 10^{12}$ and $1.5 \times 10^{13}\,cm^{-2}$. Recently, 1 kV operation of FETs has also been demonstrated using this $Al_2O_3$ passivation technique.[14] Similarly, $Al_2O_3$ has been used to encapsulate previously identified $NO_2$ surface accepter states,[15] achieving higher temperature operation.[16] Although this work has yielded very promising device performance, the exact mechanism that is responsible for the hole accumulation of diamond passivated by $Al_2O_3$ is still a point of investigation. Similar work involving ALD deposition of $Al_2O_3$ and $HfO_2$ has been explored for use in H-diamond MOSFETs.[17]

Previous work has demonstrated the transition metal oxide $MoO_3$ to be a promising candidate for surface transfer doping of H-diamond,[18,19] showing a significant increase in carrier concentration and improvement in temperature stability over atmospheric transfer doping. In this study, we present $V_2O_5$ as an alternative transition metal oxide for the surface transfer doping of H-diamond. In comparison with

a)Electronic mail: k.crawford.2@research.gla.ac.uk
b)Electronic mail: d.qi@latrobe.edu.au

 

$MoO_3$, $V_2O_5$ also possesses a sufficiently high electron affinity (EA ~ 6.3 eV,[20]) to potentially induce surface transfer doping in H-diamond (Figure 1). Indeed, both $MoO_3$ and $V_2O_5$ have recently been shown to also induce transfer doping in thin film graphene structures.[20] Both the doping efficiency and the stability in air of $V_2O_5$ outperform that of $MoO_3$,[20–22] suggesting that $V_2O_5$ may provide a more attractive transfer doping solution for application in diamond FET technology.

The experimental work in this study was carried out in two stages using (i) 4.7 $mm^2$ boron doped single crystal diamond[19] grown via chemical vapour deposition (CVD) on a type IIa (001) CVD sample (Element Six) and (ii) two intrinsic single crystal CVD diamonds[23] grown on Ib HPHT diamond substrates: stage 1—Photoemission spectroscopy (PES) of the H-diamond/$V_2O_5$ interface and stage 2—Electrical characterisation of the subsurface hole channel in the diamond formed by $V_2O_5$ and air-induced surface transfer doping.

In Stage 1, for enabling PES studies of the interfacial electronic structures, a 300 nm-thick boron-doped epitaxial layer with a boron concentration in the order of $10^{18}$ $cm^{-3}$ was grown by microwave plasma assisted CVD on one of the diamond substrates used for this study. Details on the epitaxial growth of the boron-doped adlayer can be found in Ref. 19. Prior to PES measurements, the diamond sample was cleaned thoroughly by boiling in an acid mixture ($H_2SO_4$:$HNO_3$:$HClO_4$ = 1:1:1) to remove any metallic and organic adsorbates. Hydrogen-termination was then achieved using a dedicated microwave hydrogen plasma reactor with the diamond substrate kept at around 800 °C to produce a hydrogen-terminated 2 × 1 reconstructed surface. All subsequent preparations and PES measurements were performed in an ultra-high vacuum (UHV) chamber with a base pressure of $1 \times 10^{-10}$ mbar fitted at the end-station of SINS beamline at the Singapore Synchrotron Light Source (SSLS).[24] The sample was annealed *in-situ* at 400 °C for about 10 min to remove any residual surface adsorbates and/or remnant hydrocarbon molecules from the hydrogen plasma process, whilst leaving the hydrogen termination intact.[25,26] After cooling-down to room temperature, the deposition of $V_2O_5$ was carried out by subliming from a standard Knudsen-cell set at 590 °C. The nominal thickness of $V_2O_5$ thin films was estimated from the attenuation of the bulk diamond C 1*s* peak intensity after each deposition.

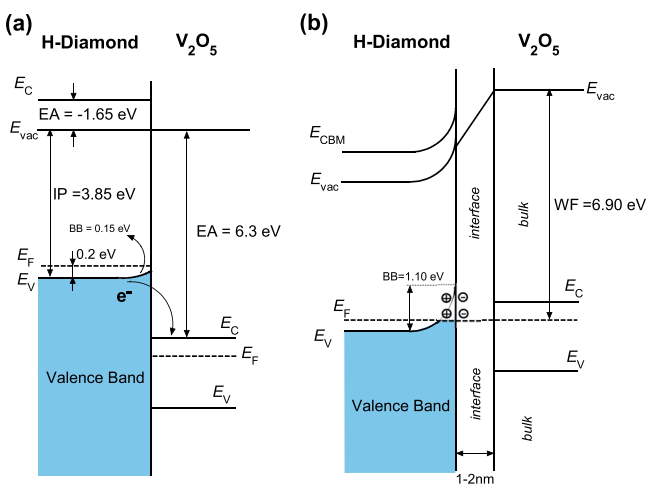


FIG. 1. Schematic energy level diagram before and after surface transfer doping using $V_2O_5$ as a surface acceptor. Other than the electron affinity (EA) of $V_2O_5$, all energy levels are determined by PES following established procedures.[11] IP represents ionization potential. EA represents electron affinity and BB represents band bending. The uncertainty of the position of the energy level is 0.10 eV.

PES spectra of the C 1*s* and V 2*p* were recorded by a Scienta R4000 electron energy analyzer at normal emission geometry using photon energies of 350 eV and 650 eV, respectively. The binding energies of all PES spectra were calibrated and referenced to the Fermi energy of a sputtered gold foil in electrical contact with the diamond sample. The work function was measured by recording the secondary electron emission in the low kinetic energy region with an incoming photon energy set to 60 eV. A −9 V bias was applied to the sample in order to overcome the work function of the analyzer.

The diamond surface band bending, which can be revealed by the rigid shifts in diamond C 1*s* component, is a direct signature of hole accumulation in diamond induced by surface transfer doping.[9,11] The evolution of diamond C 1*s* PES spectra, as a function of $V_2O_5$ coverage, is shown in Figure 2(a). Immediately after the deposition of 0.4 Å $V_2O_5$, a rigid shift of 0.30 eV of the diamond C1s peak to the lower binding energy side is clearly observed, consistent with an upward band bending expected after electron transfer from the diamond valence band to surface acceptors. The diamond peak continues to shift to the lower binding energy side with subsequent $V_2O_5$ deposition and becomes almost unchanged with $V_2O_5$ coverage beyond 18 Å as also shown in Figure 2(d). The total binding energy shift as a result of $V_2O_5$ deposition is 0.95 ± 0.05 eV, suggesting a further upward band bending of the same amount towards the diamond surface (Figure 1(b)). The band bending amount, and thus the areal hole concentration on the diamond surface, is comparable with that for $MoO_3$ doped diamond surface,[19] suggesting that $V_2O_5$ is at least as effective in surface transfer doping of diamond as $MoO_3$.

On the $V_2O_5$ side, negatively charged $V_2O_5$ interfacial clusters are identified in the V 2p spectra by performing least square peak fitting routine to deconvolute the $V^{4+}$ species (Figure 2(b)).[27] The $V^{4+}/V^{5+}$ ratio is found to be reduced significantly from 0.27 for 0.8 Å $V_2O$ to less than 0.08 for 6.4 Å and eventually becomes 0 within the instrumental detection limit for thickness beyond 51 Å. This thickness dependent $V^{4+}/V^{5+}$ intensity ratio corroborates the interfacial nature of the negatively charged $V_2O_5$ species as expected from the surface transfer doping model[10,11] and clearly rules out the possibility of the formation of reduced $V_2O_5$ species due to oxygen vacancies during the deposition process. Finally, the work function, as indicated by the secondary electron cut-off (SECO) in Figure 2(c) (also see Figure 2(e)), increases from 3.80 eV for clean H-diamond to 6.90 eV for bulk $V_2O_5$, as a result of the interface dipole built from the interfacial charge separation.

In Stage 2, unlike the diamond sample used for PES analysis which utilised a boron doped surface layer to eliminate charging effects, intrinsic diamond samples sourced without any additional doping were used for this electrical characterisation study. Details on the epitaxial growth of the intrinsic layer are reported in Ref. 23. Prior to hydrogen termination, two nominally identical samples were cleaned in

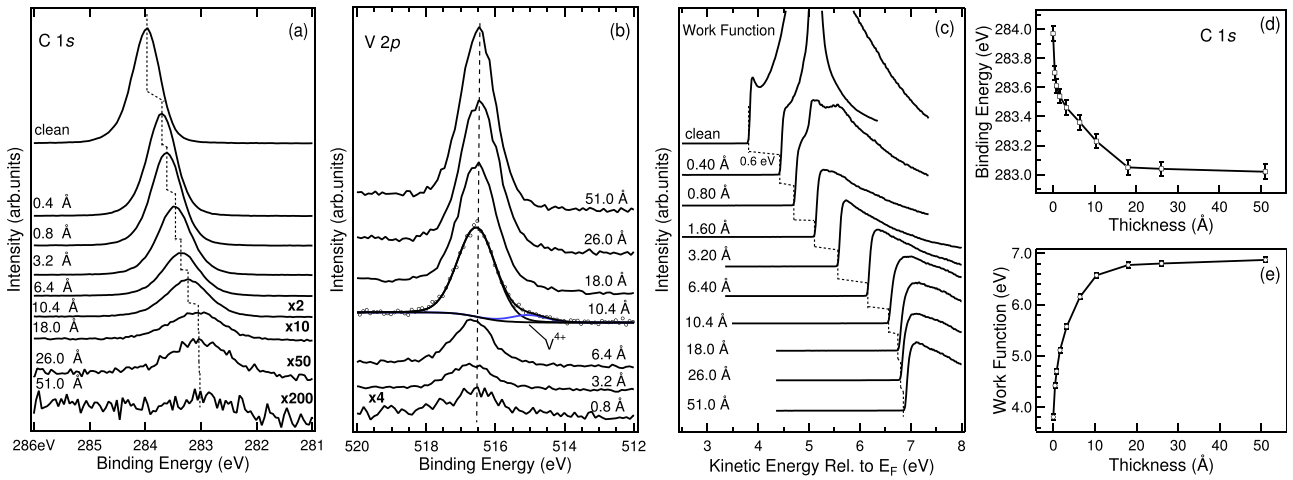


FIG. 2. PES core level spectra of (a) C 1s with photon energy of 350 eV, (b) V $2p_{3/2}$ with photon energy of 650 eV, and (c) secondary electron cut-off indicating work function using photon energy of 60 eV for hydrogen-terminated diamond with increasing $V_2O_5$ thickness. The diamond C 1s peak position and work function as a function of $V_2O_5$ thickness are plotted in (d) and (e), respectively. An example of the least square peak fitting (blue line) for the V $2p_{3/2}$ peaks is shown for 10.4 Å of $V_2O_5$.

$HNO_3$:HCl followed by $H_2SO_4$:$HNO_3$ to remove any metallic and organic adsorbents. These were then treated with hydrogen plasma for 30 min at a substrate temperature of 600 °C to terminate the surface with hydrogen. Van der Pauw (VDP) test structures were fabricated on each by applying silver paste to the corners of the samples. For the purpose of making "large area" ohmic contacts to H-diamond for our VDP structures, silver contacts show a sufficiently low resistance and linear response.[28] Use of this simplified VDP structure minimises the risk of incurring contamination of the diamond surface using standard processing techniques, e.g., exposure to resists, chemicals, and electron beam. One sample was then baked at 400 °C for 1 h *in situ* to remove any atmospheric molecules from the H-diamond surface before 100 nm of $V_2O_5$ was thermally evaporated without exposing the sample to atmosphere post *in situ* anneal. This annealing stage is required to ensure that any observable transfer doping is induced by the $V_2O_5$ only and is not attributed to any residual encapsulated atmospheric species on the H-diamond surface.

Hall measurements were taken for this sample in an air environment before and after encapsulation with $V_2O_5$ using a Nanometrics HL5500 Hall measurement system. This yielded values for the sheet resistance, hole mobility, and carrier concentration, when the H-diamond surface was initially exposed to air and then encapsulated with $V_2O_5$ (Table I).

Due to the dependence on the variable and largely uncontrollable atmospheric surface layer for surface transfer doping in air-exposed H-diamond, reported electrical properties for the resultant hole conducting channel vary substantially.[29] Typical values for areal hole density have been found to vary between $10^{12}$ and $10^{13}$ cm$^{-2}$ at room temperature for polycrystalline and single crystal CVD films alike. Mobility has also been shown to vary with values of 30–120 cm$^2$/V s typical. In this experiment, the results show that utilising $V_2O_5$ as a surface acceptor material generated a six fold increase in carrier concentration with a final value of $1.8 \times 10^{13}$ cm$^{-2}$ in comparison to the air induced value of $3 \times 10^{12}$ cm$^{-2}$. Subsequently, sheet resistance was almost halved and mobility fell from 118 to 37 cm$^2$/V s. The final value of carrier concentration seen here is very close to that we reported elsewhere for $MoO_3$ surface transfer doping, which has a similar value of EA.[19] Further optimisation of the processing conditions for these oxide:H-diamond systems, such as hydrogen termination, surface roughness, and oxide growth, may yield higher carrier densities within the diamond and hence requires further investigation. The mechanism by which mobility is reduced is not well understood at present, though is often correlated with higher carrier concentration, possibly due to increased coulomb scattering at the interface.[30] Similar reduction in mobility was also observed after increased carrier concentration induced by $MoO_3$.[18,19]

TABLE I. Electrical transport characteristics of diamond before and after $V_2O_5$ deposition.

| | Sheet resistance (kΩ/□) | Mobility (cm$^2$/V s) | Sheet carrier concentration (cm$^{-2}$) |
|---|---|---|---|
| Air induced doping | 17.8 | 118.0 | $3.0 \times 10^{12}$ |
| After $V_2O_5$ deposition | 9.5 | 37.2 | $1.8 \times 10^{13}$ |

To verify the high resistivity of standalone $V_2O_5$ films, 100 nm of $V_2O_5$ was deposited simultaneously onto an insulating SiN substrate and electrically characterised. This demonstrated no measureable current through the oxide above the noise floor of the measurement system (~100 nA).

Further Hall measurements were performed between room temperature and 300 °C in atmosphere on the $V_2O_5$ encapsulated sample and on the second VDP test sample that remained unencapsulated with its surface exposed to air. These results which are plotted in Figure 3 show the hole density of the $V_2O_5$ doped sample to be largely stable up to ~250 °C with a gradual increase in sheet resistance at higher temperatures as carrier concentration begins to decrease above 250 °C. Mobility is observed to vary marginally for this sample but generally decreases slowly with increased temperature. These results are in sharp contrast to those attained for the air-doped sample, which exhibits a rapid increase in sheet resistance above ~60 °C due to a combined reduction of both carrier concentration and mobility. The

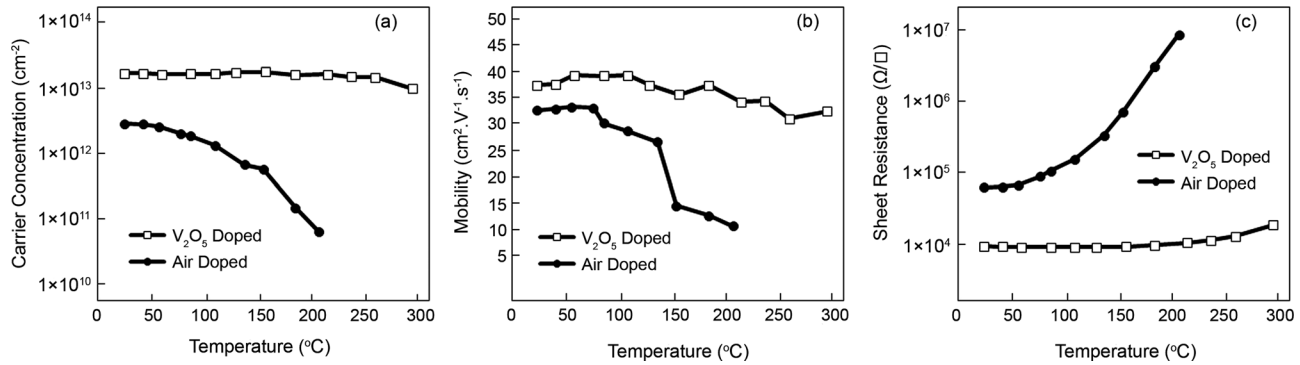


FIG. 3. Hall measurements for both $V_2O_5$ and air doped H-terminated diamond plotted against temperature: (a) carrier concentration, (b) mobility, and (c) sheet resistance.

observed decrease in carrier concentration for this sample is readily explained by desorption of the airborne molecular species from the air-exposed H-diamond surface with increased temperature.[3] The exact mechanism by which the mobility is reduced with increased temperature for the air-doped sample is more difficult to explain but may be related to reduced screening of interface scattering effects as the carrier density is reduced. Unfortunately, no Hall data are available for the air-doped sample above ~200 °C as its electrical properties were degraded to the point that it became unmeasurable by our measurement system.

In conclusion, the transition metal oxide $V_2O_5$ has been demonstrated to induce surface transfer doping on hydrogen-terminated diamond as verified by both photoemission spectroscopy and Hall measurement. These results show excellent potential in comparison with air-induced transfer doping, with good stability when exposed to atmosphere at elevated temperatures up to ~250 °C. While the composition of atmospheric molecules on the surface is volatile and uncontrollable, surface transfer doping utilising oxide-based surface acceptors represent a viable solid-state approach to enable diamond-based surface conducting electronics. Furthermore, while the band bending in diamond and total work function shift are comparable to those of $MoO_3$, $V_2O_5$ may prove to be a more stable and hence desirable solution for implementation in surface-transfer doped diamond electronic devices. Further investigation into the stability of these materials and their potential integration into diamond field-effect transistors is therefore warranted.

The authors wish to thank staff at the James Watt Nanofabrication Centre for their assistance with this work. D.-C.Q. acknowledges the support of the Disciplinary Research Program (DRP) of the La Trobe University and the Australian Research Council (Grant No. DP150101673). LC is grateful for the support of the National Natural Science Foundation of China (Grant Nos. 11574317 and 21503233). This work was partly performed at SSLS under NUS Core Support C-380-003-003-001. The authors acknowledge the beam-time support from Dr. Xiaojiang Yu and Professor Mark Breese.

[1]C. J. H. Wort and R. S. Balmer, Mater. Today **11**, 22 (2008).
[2]W. Chen, D. Qi, X. Gao, and A. T. S. Wee, Prog. Surf. Sci. **84**, 279 (2009).
[3]F. Maier, M. Riedel, B. Mantel, J. Ristein, and L. Ley, Phys. Rev. Lett. **85**, 3472 (2000).
[4]K. Ueda, M. Kasu, Y. Yamauchi, T. Makimoto, M. Schwitters, D. J. Twitchen, G. A. Scarsbrook, and S. E. Coe, IEEE Electron Device Lett. **27**, 570 (2006).
[5]K. Hirama, H. Takayanagi, S. Yamauchi, Y. Jingu, H. Umezawa, and H. Kawarada, Tech. Dig. -Int. Electron Device Meet. **2007**, 873.
[6]S. A. O. Russell, S. Sharabi, A. Tallaire, and D. A. J. Moran, IEEE Electron Device Lett. **33**, 1471 (2012).
[7]M. Kasu, K. Ueda, Y. Yamauchi, A. Tallaire, and T. Makimoto, Diamond Relat. Mater. **16**, 1010 (2007).
[8]M. Kasu, K. Ueda, H. Ye, Y. Yamauchi, S. Sasaki, and T. Makimoto, Electron. Lett. **41**, 1249 (2005).
[9]P. Strobel, M. Riedel, J. Ristein, and L. Ley, Nature **430**, 439 (2004).
[10]M. T. Edmonds, M. Wanke, A. Tadich1, H. M. Vulling, K. J. Rietwyk, P. L. Sharp, C. B. Stark, Y. Smets, A. Schenk, Q. H. Wu, L. Ley, and C. I. Pakes, J. Chem. Phys. **136**, 124701 (2012).
[11]D. Qi, W. Chen, X. Gao, L. Wang, S. Chen, K. P. Loh, and A. T. S. Wee, JACS **129**, 8084 (2007).
[12]P. Strobel, J. Ristein, L. Ley, K. Seppelt, I. V. Goldt, and O. Boltalina, Diamond Relat. Mater. **15**, 720 (2006).
[13]A. Daicho, T. Saito, S. Kurihara, A. Hiraiwa, and H. Kawarada, J. Appl. Phys. **115**, 223711 (2014).
[14]H. Kawarada, T. Yamada, D. Xu, H. Tsuboi, T. Saito, and A. Hiraiwa, Tech. Dig. -Int. Electron Device Meet. **2014**, 11.2.1.
[15]Y. Takagi, K. Shiraishi, M. Kasu, and H. Sato, Surf. Sci. **609**, 203 (2013).
[16]K. Hirama, H. Sato, Y. Harada, H. Yamamoto, and M. Kasu, IEEE Electron Device Lett. **33**, 1111 (2012).
[17]J. W. Liu, M. Y. Liao, M. Imura, and Y. Koide, Appl. Phys. Lett. **101**, 252108 (2012).
[18]M. Tordjman, C. Saguy, A. Bolker, and R. Kalish, Adv. Mater. Interfaces **1**, 1300155 (2014).
[19]S. A. O. Russell, L. Cao, D. Qi, A. Tallaire, K. G. Crawford, A. T. S. Wee, and D. A. J. Moran, Appl. Phys. Lett. **103**, 202112 (2013).
[20]A. Kuruvila, P. R. Kidambi, J. Kling, J. B. Wagner, J. Robertson, S. Hofmann, and J. Meyer, J. Mater. Chem. C **2**, 6940 (2014).
[21]I. Irfan, H. J. Ding, Y. L. Gao, D. Y. Kim, J. Subbiah, and F. So, Appl. Phys. Lett. **96**, 073304 (2010).
[22]J. Q. Zhong, H. Y. Mao, R. Wang, J. D. Lin, Y. B. Zhao, J. L. Zhang, D. G. Ma, and W. Chen, Org. Electron. **13**, 2793 (2012).
[23]C. Verona, W. Ciccognani, S. Colangeli, F. Di Pietrantonio, E. Giovine, E. Limiti, M. Marinelli, and G. Verona-Rinati, IEEE Trans. Electron Devices **62**, 1150 (2015).
[24]X. Yu, O. Wilhelmi, H. O. Moser, S. V. Vidyaraj, X. Gao, A. T. S. Wee, T. Nyunt, H. Qian, and H. Zheng, J. Electron Spectrosc. Relat. Phenom. **144–147**, 1031 (2005).
[25]L. Ley, J. Ristein, F. Meier, M. Riedel, and P. Strobel, Physica B **376–377**, 262 (2006).
[26]D. Qi, J. Sun, X. Gao, L. Wang, S. Chen, K. P. Loh, and A. T. S. Wee, Langmuir **26**, 165 (2010).
[27]M. C. Biesinger, L. W. M. Lau, A. R. Gerson, and R. St. C. Smart, Appl. Surf. Sci. **257**, 887 (2010).
[28]M. C. Rossi, F. Spaziani, S. Salvatori, and G. Conte, Phys. Status Solidi **199**, 71 (2003).
[29]N. Jiang and T. Ito, J. Appl. Phys. **85**, 8267 (1999).
[30]H. J. Looi, R. B. Jackman, and J. S. Foord, Appl. Phys. Lett. **72**, 353 (1998).